Copyright by the Hindawi Publishing Corporation. Nenggen Ding and Saied Taheri, "Application of Recursive Least Square Algorithm on Estimation of Vehicle Sideslip Angle and Road Friction," Mathematical Problems in Engineering, vol. 2010, Article ID 541809, 18 pages, 2010. doi:10.1155/2010/541809

Hindawi Publishing Corporation
Mathematical Problems in Engineering
Volume 2010, Article ID 541809, 18 pages
doi:10.1155/2010/541809

Research Article

Application of Recursive Least Square Algorithm on Estimation of Vehicle Sideslip Angle and Road Friction

Nenggen Ding[1] and Saied Taheri[2]

[1] *Department of Automobile Engineering, Beihang University, 37 Xueyuan Road, Haidian District, Beijing 100083, China*
[2] *Mechanical Engineering Department, Virginia Polytechnic Institute and State University, Blacksburg, VA 24060, USA*

Correspondence should be addressed to Nenggen Ding, dingng@buaa.edu.cn

Received 3 August 2009; Revised 5 December 2009; Accepted 10 February 2010

Academic Editor: J. Rodellar

Copyright © 2010 N. Ding and S. Taheri. This is an open access article distributed under the Creative Commons Attribution License, which permits unrestricted use, distribution, and reproduction in any medium, provided the original work is properly cited.

A recursive least square (RLS) algorithm for estimation of vehicle sideslip angle and road friction coefficient is proposed. The algorithm uses the information from sensors onboard vehicle and control inputs from the control logic and is intended to provide the essential information for active safety systems such as active steering, direct yaw moment control, or their combination. Based on a simple two-degree-of-freedom (DOF) vehicle model, the algorithm minimizes the squared errors between estimated lateral acceleration and yaw acceleration of the vehicle and their measured values. The algorithm also utilizes available control inputs such as active steering angle and wheel brake torques. The proposed algorithm is evaluated using an 8-DOF full vehicle simulation model including all essential nonlinearities and an integrated active front steering and direct yaw moment control on dry and slippery roads.

1. Introduction

The performance of a vehicle active safety system depends on not only the control algorithm, but also on the estimation of some key states if they can not directly be measured. Among these states to be estimated online, vehicle sideslip angle and tire-road friction coefficient have been extensively studied in the literature. It is noted that road friction is also used for determination of target response to driver's steering inputs in the entire range of operation.

There are several strategies [1–5] for estimation of sideslip angle and road friction, such as Kalman filter (KF), RLS algorithms, closed-loop feedback observers [2] and sliding

mode observers [6]. Gustafsson and many others [7–10] designed observers based on tire-road force models and single-track vehicle models. In [1], Yi et al. designed an observer of tire-road friction coefficient using RLS methods for vehicle collision warning/avoidance system. Wenzel et al. [11], and Baffet et al. [12], independently proposed a dual extended Kalman filter (DEKF) for estimation of vehicle states and parameters which is intended for various active chassis control systems. From the viewpoint of online estimation, the DEKF is too complex to be used with the current systems, due to the limited computational authority of microprocessors and availability of only a few sensors.

A common feature of most state observer and KF/RLS based algorithms for estimation of sideslip angle is that they rely heavily on an accurate tire model, which may vary during vehicle operation. To overcome the limitation, Hac and Simpson [2], combined the state estimation method based on vehicle dynamic model with a closed-loop nonlinear observer to estimate yaw rate and sideslip angle of the vehicle. This resulted in good estimates for maneuvers on high-friction roads using "pseudomeasurement" of yaw rate as preliminary estimate to supply additional feedback to the observer, which gets rid of the sensor for direct measurement of yaw rate. However, sideslip angle cannot be estimated with enough accuracy on very low-friction roads. Cheli et al. [13], estimated sideslip angle as a weighted mean of the results provided by a kinematic formulation and those obtained through a state observer based on vehicle single-track model. The basic idea is to make use of the information provided by the kinematic formulation during a transient maneuver to update the single-track model parameters (tire cornering stiffness).

In [14], tire-road friction estimation (TRFE) methodologies are classified as four types. The first approach is slip-based and the other three use dedicated optical, acoustic [15, 16], or strain gage type sensors [7, 15–18]. Slip-based approaches use wheel slip calculated based on the difference between the wheel velocities of driven and nondriven wheels at normal driving conditions [3, 14, 19]. The slip-based approach can be further extended to model-based friction estimation [1, 8, 12, 14], in which wheel dynamics and/or brake pressure model, and vehicle longitudinal and/or lateral dynamics, are employed.

The main idea of most slip-based friction estimation approaches is to predict the maximum friction based on the collected low-slip and low-friction data at normal driving, where normally acceleration/deceleration is less than $0.2\,g$ [3] and slip ratios are rarely greater than 5%. In these cases, maximum tire-road friction is estimated according to the slope at the low values of slip/friction curve of the driven wheels, which is mainly determined by the tire carcass stiffness rather than the road condition and thus quite sensitive to tire type, inflation pressure, tire wear, and possibly vehicle configuration [19].

Estimation of vehicle sideslip angle relies heavily on an accurate tire model, but the computing power required in such detailed models easily exceeds the control cycle time. For example, the famous Magic Formula tire model can very accurately represent the force and moment properties. However, due to trigonometric and exponential functions associated with such formulation with several associated coefficients, the time required for online calculation, far exceeds the control cycle time. On the other hand, if tire and vehicle dynamic models do not include the required details, estimation accuracy will be lost. Consequently, several efficient and accurate tire models with simpler expressions of tire forces have been investigated in the literature. In other words, a compromise between accuracy and complexity of tire model is required for online implementation.

In this paper, an RLS algorithm is proposed to estimate sideslip angle and road friction for online application during activation of active front steering and direct yaw moment control. Two main means are adopted to reduce the computational time of the algorithm.

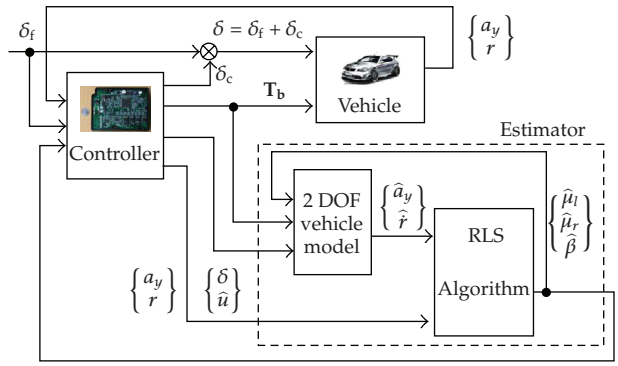

Figure 1: Scheme of the proposed algorithm for sideslip angle and road friction estimation.

The first one is use of a modified Dugoff tire model, for which simple expressions of tire forces are used and parametric differences with respect to tire normal forces can be easily functionalized using polynomials. The second one is online linearization of the model and iterative computation for the proposed algorithm which are distributed to different control cycles without sacrificing estimation accuracy. A significant merit of the algorithm lies in the fact that it can provide estimates with reasonable accuracy without additional sensors. It makes adequate use of the data available through the control logic for correction steering angle and wheel brake torques. Comparison between estimated results and simulation data using Matlab/Simulink and an 8-DOF full vehicle model shows that the proposed algorithm is promising for practical use in active safety systems.

2. Algorithm Description

The algorithm considered in this paper is intended for real-time online estimation of sideslip angle and road friction for the vehicle stability control systems using active front steering and direct yaw moment control. Due to the limited computational authority of microprocessors used in vehicle control systems, the algorithm should not be too complex. A simple two-degrees-of-freedom (DOF) vehicle model is used to develop the estimation algorithm. Shown in Figure 1 is the scheme of the proposed algorithm for sideslip angle and road friction estimation.

The estimator in Figure 1 consists of the vehicle model and the RLS algorithm. All the inputs of the estimator are from the controller (i.e., electric control unit, or ECU), either directly measured by sensors or estimated by the control algorithm. Here, it is assumed that such typical sensors as those for lateral acceleration and yaw rate of the vehicle, steering wheel angle, and wheel speeds are used. Vehicle speed is estimated using the wheel speeds.

In the vehicle model, tire forces are computed according to the estimated vehicle states $\hat{u}$ and $\hat{\beta}$, estimated road friction $\hat{\mu}_l$ and $\hat{\mu}_r$, and control inputs of steering angle δ and brake torque "vector" $\mathbf{T_b}$. The lateral and yaw accelerations are then estimated and used in the RLS algorithm. Errors of lateral acceleration and yaw acceleration of the vehicle are computed according to inputs from the vehicle model and the controller, and the RLS algorithm uses these errors to recursively estimate the sideslip angle and road friction.

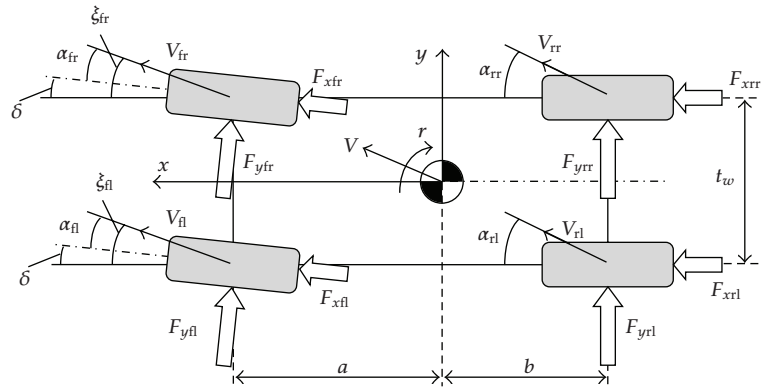

Figure 2: A two DOF vehicle model with four wheels.

2.1. A 2-DOF Vehicle Model

Shown in Figure 2 is the 2-DOF vehicle model with 4 wheels. The model is intended for online computation of lateral and yaw accelerations based on vehicle states and road friction conditions. Equations governing the lateral and yaw motion of the vehicle are as follows

$$\begin{aligned} m(\dot{u} - rv) &= F_{xf}\sin(\delta) + F_{yf}\cos(\delta) + F_{yr}, \\ I_z\dot{r} &= aF_{xf}\sin(\delta) + aF_{yf}\cos(\delta) - bF_{yr}, \\ &\quad + \frac{t_w}{2}\left[(F_{xfl} - F_{xfr})\cos(\delta) - (F_{yfl} - F_{yfr})\sin(\delta) + (F_{xrl} - F_{xrr})\right]. \end{aligned} \tag{2.1}$$

Note that the vehicle velocity at the center of gravity, V, is the resultant vector of longitudinal speed u and lateral speed v. Tire slip angles can be determined according to kinematic relationships shown in Figure 2 as follows:

$$\begin{aligned} \alpha_{fl} &= \xi_{fl} - \delta = \tan^{-1}\frac{v + ra}{u + rt_w/2} - \delta, \\ \alpha_{fr} &= \xi_{fr} - \delta = \tan^{-1}\frac{v + ra}{u - rt_w/2} - \delta, \\ \alpha_{rl} &= \xi_{rl} = \tan^{-1}\frac{v - rb}{u + rt_w/2}, \\ \alpha_{rr} &= \xi_{rr} = \tan^{-1}\frac{v - rb}{u - rt_w/2}. \end{aligned} \tag{2.2}$$

Wheel load transfer is included in calculation of tire normal force as follows:

$$F_{zij} = F_{zsij} \pm \frac{h_g m\hat{a}_x}{2L} \mp \frac{h_g m a_y}{2t_w}, \quad i = \mathrm{f,r};\ j = \mathrm{l,r}, \tag{2.3}$$

where + and − need to be properly selected for each specific tire, and $\hat{a}_x$ is the estimated longitudinal acceleration according to the estimated longitudinal speed. Although lateral load transfer should be distributed between the two axles according to suspension roll stiffness and some other factors, here only the average lateral inertia force is included and distributed.

During a typical intervention of AFS/DYC, the tires often operate at or near the friction limit and combined-slip conditions may arise. Therefore, a nonlinear tire model capable of simulating the friction ellipse phenomena is required. A modified Dugoff tire model is used here for the estimator. First, lateral tire forces at pure-slip conditions are calculated using the modified Dugoff model and longitudinal forces are determined from the brake torques. Then, the lateral forces are further amended according to the magnitude of the longitudinal force. Variation of tire-road friction with respect to slip is included in the calculation of the lateral forces.

The pure-slip lateral force is first calculated for dry asphalt road with a nominal tire-road friction coefficient $\mu_0 = 1.0$ and then is adjusted for the estimated friction coefficient $\hat{\mu}$($\hat{\mu}_\mathrm{l}$ or $\hat{\mu}_\mathrm{r}$). Calculation of F_{0y} can be summarized as follows:

$$\begin{gathered}
C_\alpha = c_1 {F_z}^2 + c_2 F_z + c_3, \qquad F_{y\mathrm{p}} = c_4 {F_z}^2 + c_5 F_z, \\
F_{y\mathrm{s}} = c_6 F_z + c_7, \qquad S_\alpha = \min(|\tan\alpha|, 1), \\
\mu_0 F_z = c_8 F_{y\mathrm{p}}(1 - S_\alpha) + F_{y\mathrm{s}} S_\alpha, \qquad \lambda = \frac{\mu_0 F_z}{2C_\alpha \tan\alpha}, \\
f(\lambda) = \begin{cases} (2-\lambda)\lambda, & \lambda < 1, \\ 1, & \lambda \geq 1, \end{cases} \qquad F_{0y} = \frac{\hat{\mu}}{\mu_0} C_\alpha \tan(\alpha) f(\lambda),
\end{gathered} \tag{2.4}$$

where the coefficients c_i's ($i = 1 \sim 8$) in (2.4) can be determined according to tire test data or drawn from other tire models which have a high accuracy but are not suitable for online computation, and $\tan\alpha$ can be determined from (2.2) as follows:

$$\begin{aligned}
\tan(\alpha_{\mathrm{fl}}) &= \frac{(v + ra) - (u + rt_\mathrm{w}/2)\delta}{(u + rt_\mathrm{w}/2) + (v + ra)\delta}, \\
\tan(\alpha_{\mathrm{fr}}) &= \frac{(v + ra) - (u - rt_\mathrm{w}/2)\delta}{(u - rt_\mathrm{w}/2) + (v + ra)\delta}, \\
\tan(\alpha_{\mathrm{rl}}) &= \frac{v - ra}{u + rt_\mathrm{w}/2}, \\
\tan(\alpha_{\mathrm{rr}}) &= \frac{v - rb}{u - rt_\mathrm{w}/2},
\end{aligned} \tag{2.5}$$

where $\tan\delta$ has been set equal to δ due to the fact that, during AFS/DYC intervention, the total steering angle at front wheels is not likely to exceed 20° (the relative error at 20° is only approximately 4.1%).

The coefficient c_8 is used to compensate for overlimitation of tire force value at large slip rates in the original Dugoff tire model. Shown in Figure 3 are some examples of lateral forces using the modified Dugoff model and a Magic Formula model, where the coefficients

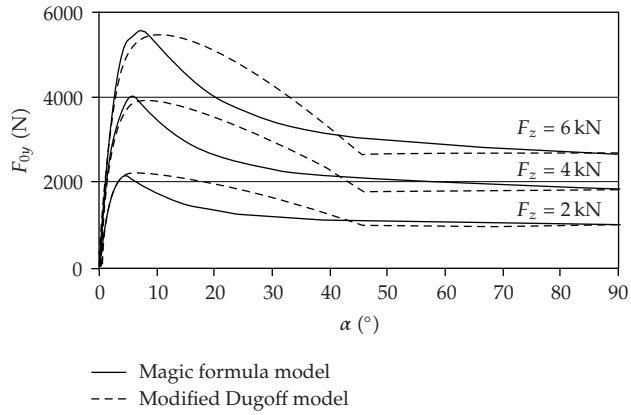

Figure 3: Tire forces at pure-slip conditions based on a Magic Formula model and a modified Dugoff model.

in the former are drawn from the latter. When slip angles are small or very large, the two models are close. For a real vehicle, the slip angle is normally less than 10°, and thus the modified model is suitable for practical use. However, the computational power required for the modified Dugoff model using (2.4) and (2.5) is much less than that of Pacejka Magic Formula model.

When DYC is activated, brake torque is applied on some of the wheels. For simplification, tire longitudinal forces are calculated using the following equation

$$F_x = -F_b = -\frac{T_b}{R_w}, \tag{2.6}$$

where T_b is the brake torque commanded by the controller. Since a wheel slip controller is usually incorporated in the AFS/DYC control system, the above simplification is made based on the following assumptions:

(1) The target brake torque can always be realized without delay;

(2) The longitudinal slip rate $\kappa$is constant during activation of DYC.

Further, κ is assumed to be 0.2 for determination of the final lateral forces at combined-slip conditions as follows

$$F_y = F_{0y}\frac{S_\alpha}{\sqrt{\kappa^2 + S_\alpha^2}}. \tag{2.7}$$

In order to reduce the computational requirements, (2.8) was fitted to (2.7) where κ takes a fixed value of 0.2:

$$F_y = \begin{cases} F_{0y}S_\alpha(5.21 - 8.24S_\alpha) & \text{if } S_\alpha \le 0.25, \\ F_{0y}(0.7231 + 0.2575S_\alpha) & \text{if } S_\alpha > 0.25. \end{cases} \tag{2.8}$$

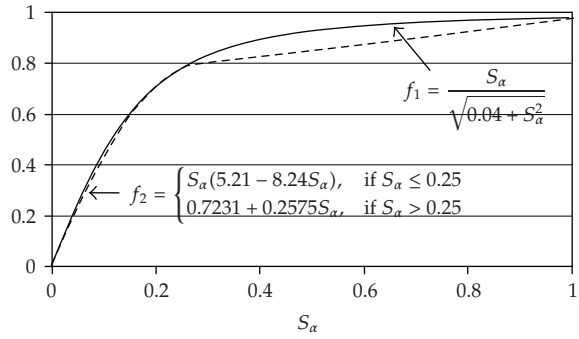

Figure 4: Comparison between two functions.

When slip angle is less than 10° (this is almost always true as mentioned above), or equivalently $S_\alpha = 0.1763$, the results using (2.7) and (2.8) are very close as shown in Figure 4.

2.2. RLS Algorithm

The recursive least square algorithm introduced here was developed based on a simple two-degrees-of-freedom vehicle model. Due to the nonlinearities involved in the equations, online linearization becomes a dynamic part of the algorithm.

As shown in Figure 1, tire-road nominal friction coefficients for the left and right sides and the sideslip angle at the vehicle's center of gravity need to be estimated. Since both vehicle lateral acceleration a_y and yaw acceleration $\dot{r}$ are nonlinear functions of the estimated parameters, linearization of these functions is required when employing the RLS algorithm. Let

$$\begin{aligned} a_y &= g_1(\mu_l, \mu_r, \beta), \\ \dot{r} &= g_2(\mu_l, \mu_r, \beta), \end{aligned} \tag{2.9}$$

and define the functions at a given point $\mathbf{p}_0 = [\mu_{l0}, \mu_{r0}, \beta_0]^T$ as follows:

$$\begin{aligned} a_{y0} &= g_1(\mu_{l0}, \mu_{r0}, \beta_0), \\ \dot{r}_0 &= g_2(\mu_{l0}, \mu_{r0}, \beta_0). \end{aligned} \tag{2.10}$$

At this point, functions g_1 and g_2 can be linearized as follows

$$\begin{aligned} a_y &= a_{y0} + \left.\frac{\partial g_1}{\partial \mu_l}\right|_{\mathbf{p}_0} \Delta\mu_l + \left.\frac{\partial g_1}{\partial \mu_r}\right|_{\mathbf{p}_0} \Delta\mu_r + \left.\frac{\partial g_1}{\partial \beta}\right|_{\mathbf{p}_0} \Delta\beta, \\ \dot{r} &= \dot{r}_0 + \left.\frac{\partial g_2}{\partial \mu_l}\right|_{\mathbf{p}_0} \Delta\mu_l + \left.\frac{\partial g_2}{\partial \mu_r}\right|_{\mathbf{p}_0} \Delta\mu_r + \left.\frac{\partial g_2}{\partial \beta}\right|_{\mathbf{p}_0} \Delta\beta, \end{aligned} \tag{2.11}$$

where

$$\Delta\mu_{\mathrm{l}} = \mu_{\mathrm{l}} - \mu_{\mathrm{l}0}, \qquad \Delta\mu_{\mathrm{r}} = \mu_{\mathrm{r}} - \mu_{\mathrm{r}0}, \qquad \Delta\beta = \beta - \beta_0. \tag{2.12}$$

Equation (2.11) can be rewritten as follows:

$$\begin{aligned} x_1 &= b_{11}\Delta\mu_{\mathrm{l}} + b_{12}\Delta\mu_{\mathrm{r}} + b_{13}\Delta\beta, \\ x_2 &= b_{21}\Delta\mu_{\mathrm{l}} + b_{22}\Delta\mu_{\mathrm{r}} + b_{23}\Delta\beta, \end{aligned} \tag{2.13}$$

where

$$\begin{aligned} x_1 &= a_y - a_{y0}, \\ x_2 &= \dot{r} - \dot{r}_0, \\ b_{i1} = \left.\frac{\partial g_i}{\partial \mu_{\mathrm{l}}}\right|_{\mathbf{p}_0}, &\quad b_{i2} = \left.\frac{\partial g_i}{\partial \mu_{\mathrm{r}}}\right|_{\mathbf{p}_0}, \quad b_{i3} = \left.\frac{\partial g_i}{\partial \beta}\right|_{\mathbf{p}_0}, \quad i = 1, 2. \end{aligned} \tag{2.14}$$

Now the unknown parameter vector and the state vector can be defined using the following equations:

$$\begin{aligned} \boldsymbol{\theta} &= \begin{bmatrix} \Delta\mu_{\mathrm{l}} & \Delta\mu_{\mathrm{r}} & \Delta\beta \end{bmatrix}^T, \\ \mathbf{x} &= \begin{bmatrix} x_1 & x_2 \end{bmatrix}^T. \end{aligned} \tag{2.15}$$

The state vector error can be expressed as

$$\mathbf{e}_k = \mathbf{x}_k - \mathbf{B}\widehat{\boldsymbol{\theta}}_k, \tag{2.16}$$

Where

$$\mathbf{B} = \begin{bmatrix} b_{11} & b_{12} & b_{13} \\ b_{21} & b_{22} & b_{23} \end{bmatrix}. \tag{2.17}$$

Define an index Φ with a forgetting factor λ as follows:

$$\Phi = \sum_{i=2}^{k} \lambda^{k-i} \mathbf{e}_i^T \mathbf{e}_i, \quad 0 < \lambda \leq 1. \tag{2.18}$$

By adopting the formulations given above and using the procedure in [1] for minimizing the index given by (2.18), the unknown parameters can be estimated as follows

$$\begin{aligned}\widehat{\boldsymbol{\theta}}_{k+1} &= \widehat{\boldsymbol{\theta}}_k + \mathbf{F}_{k+1}\mathbf{B}^T\left(\mathbf{x}_{k+1} - \mathbf{B}\widehat{\boldsymbol{\theta}}_k\right)\\ \mathbf{F}_{k+1} &= \frac{1}{\lambda}\left[\mathbf{F}_k - \mathbf{F}_k\mathbf{B}^T\left(\lambda\mathbf{I} + \mathbf{B}\mathbf{F}_k\mathbf{B}^T\right)^{-1}\mathbf{B}\mathbf{F}_k\right]\\ \widehat{\boldsymbol{\theta}}_1 &= \boldsymbol{\theta}_0, \quad \mathbf{F}_1 = \sigma\mathbf{I},\end{aligned} \tag{2.19}$$

where $\boldsymbol{\theta}_0$ is always set to zero (this is only specific for the problem stated here), σ is a large number, and $\mathbf{I}$ is a unit matrix with the proper dimensions.

On certain situations such that when estimated road friction coefficients or sideslip angle are far from current operating point, a new operating point is needed and linearization of the functions g_1 and g_2 need to be renewed since (2.11) or (2.13) hold only when $\|\boldsymbol{\theta}\|$ is small. Therefore, $\mathbf{p}_0$ should be renewed using $\mathbf{p}_0 + \boldsymbol{\theta}$ according to the criteria defined in the next section. Matrix $\mathbf{B}$ must be recalculated when operating point is renewed.

3. Algorithm Implementation

3.1. Numerical Implementation of Partial Derivatives

The following equations are used to compute the partial derivatives at $\mathbf{p}_0 = [\mu_{l0},\ \mu_{r0},\ \beta_0]^T$:

$$\begin{aligned}\left.\frac{\partial g_i}{\partial \mu_l}\right|_{\mathbf{p}_0} &= \frac{g_i(\mu_{l0} + \Delta\mu_{l0}, \mu_{r0}, \beta_0) - g_i(\mu_{l0} - \Delta\mu_{l0}, \mu_{r0}, \beta_0)}{2\Delta\mu_{l0}},\\ \left.\frac{\partial g_i}{\partial \mu_r}\right|_{\mathbf{p}_0} &= \frac{g_i(\mu_{l0}, \mu_{r0} + \Delta\mu_{r0}, \beta_0) - g_i(\mu_{l0},\ \mu_{r0} - \Delta\mu_{r0}, \beta_0)}{2\Delta\mu_{r0}}, \quad i = 1,2\\ \left.\frac{\partial g_i}{\partial \beta}\right|_{\mathbf{p}_0} &= \frac{g_i(\mu_{l0},\ \mu_{r0}, \beta_0 + \Delta\beta_0) - g_i(\mu_{l0},\ \mu_{r0}, \beta_0 - \Delta\beta_0)}{2\Delta\beta_0}\end{aligned} \tag{3.1}$$

Computation of the partial derivatives using (3.1) may be time-consuming. Therefore, the alternative solution adopted in this paper is distributing the computation among different control cycles to help with the limited computational authority of the microprocessor.

3.2. Criteria of Reparameterization

When any of the following conditions holds, substitute $\mathbf{p}_0$ with $\mathbf{p}_0 + \widehat{\boldsymbol{\theta}}$ and a new round of recursive process will be initiated:

$$\begin{aligned}\left\|\widehat{\boldsymbol{\theta}}\right\| &> \varepsilon,\\ n &> n_0,\end{aligned} \tag{3.2}$$

where ε is a preset small positive number, n is the number of iterative computation using (2.19) since last re-parameterization, and n_0 is a known threshold.

If the value of estimated parameters changes too quickly, restrictions for their increment are applied. In this paper, maximum increment for $\widehat{\mu}_{\mathrm{l}}$, $\widehat{\mu}_{\mathrm{r}}$ and $\widehat{\beta}$ are 0.1, 0.1, and 0.005 rad, respectively. For example, if $\widehat{\mu}_{\mathrm{l}_k} = 0.36$ and $\widehat{\mu}_{\mathrm{l}_{k+1}} = 0.49$, the value of $\widehat{\mu}_{\mathrm{l}_{k+1}}$ will be restricted to 0.46; if $\widehat{\beta}_k = 0.0023$ rad and $\widehat{\beta}_{k+1} = -0.0075$ rad, the value of $\widehat{\beta}_{k+1}$ will be restricted to -0.0027 rad. Whenever maximum increment is violated, the value for matrix $\mathbf{F}_{k+1}$ is reset as $\sigma\mathbf{I}$.

3.3. Summary of Procedure for the Estimator

To facilitate understanding of parameter estimation using the proposed RLS algorithm, the main steps of the procedure are outlined as follows.

Step 1 (determinaion of a_{y0} and $\dot{r}_0$ at $\mathbf{p}_0 = [\mu_{\mathrm{l}0}, \mu_{\mathrm{r}0}, \beta_0]^T$). a_{y0} and $\dot{r}_0$ are estimated using the 2-DOF vehicle model according to (3.3), which is rearranged from (2.1) with consideration of $a_y = \dot{u} - rv$ and using approximation for $\sin(\delta)$ and $\cos(\delta)$ under small angle assumption. $\boldsymbol{\theta}_0 = 0$ and $\sigma\mathbf{I}$ are used as the first group of parameters for a new round as in (2.19). In the following steps, (3.3) is always used if the 2-DOF vehicle model is involved.

$$\begin{aligned} \widehat{a}_y &= \frac{\left[\widehat{F}_{x\mathrm{f}}\delta + \widehat{F}_{y\mathrm{f}} + \widehat{F}_{y\mathrm{r}}\right]}{m} \\ \widehat{\dot{r}} &= \frac{\left(a\widehat{F}_{x\mathrm{f}}\delta + a\widehat{F}_{y\mathrm{f}} - b\widehat{F}_{y\mathrm{r}} + \dfrac{t_w}{2}\left[\left(\widehat{F}_{x\mathrm{fl}} - \widehat{F}_{x\mathrm{fr}} + \widehat{F}_{x\mathrm{rl}} - \widehat{F}_{x\mathrm{rr}}\right) - \left(\widehat{F}_{y\mathrm{fl}} - \widehat{F}_{y\mathrm{fr}}\right)\delta\right]\right)}{I_z} \end{aligned} \tag{3.3}$$

Go to Step 2.

Step 2 (calculation of partial derivatives with respect to μ_{l}). $g_i(\mu_{\mathrm{l}0} - \Delta\mu_{\mathrm{l}0}, \mu_{\mathrm{r}0}, \beta_0)$ and $g_i(\mu_{\mathrm{l}0} + \Delta\mu_{\mathrm{l}0}, \mu_{\mathrm{r}0}, \beta_0)$ $(i = 1, 2)$ are computed using the 2-DOF vehicle model. Then b_{11} and b_{21} are determined according to the first formula in (3.1).

Go to Step 3.

Step 3 (calculation of partial derivatives with respect to μ_{r}). Similarly, $g_i(\mu_{\mathrm{l}0}, \mu_{\mathrm{r}0} - \Delta\mu_{\mathrm{r}0}, \beta_0)$ and $g_i(\mu_{\mathrm{l}0}, \mu_{\mathrm{r}0} + \Delta\mu_{\mathrm{r}0}, \beta_0)$ $(i = 1, 2)$ are computed using the 2-DOF vehicle model. Then b_{12} and b_{22} are determined according to the second formulae in (3.1).

Go to Step 4.

Step 4 (calculation of function values of $g_i(\mu_{\mathrm{l}0}, \mu_{\mathrm{r}0}, \beta_0 - \Delta\beta_0)$). $g_1(\mu_{\mathrm{l}0}, \mu_{\mathrm{r}0}, \beta_0 - \Delta\beta_0)$ and $g_2(\mu_{\mathrm{l}0}, \mu_{\mathrm{r}0}, \beta_0 - \Delta\beta_0)$ are computed using the 2-DOF vehicle model.

Go to Step 5.

Step 5 (calculation of function values of $g_i(\mu_{l0}, \mu_{r0}, \beta_0 + \Delta\beta_0)$). $g_1(\mu_{l0}, \mu_{r0}, \beta_0 + \Delta\beta_0)$ and $g_2(\mu_{l0}, \mu_{r0}, \beta_0 + \Delta\beta_0)$ are computed using the 2-DOF vehicle model. Then b_{13} and b_{23} are determined according to the third formulae in (3.1).

Go to Step 6.

Step 6 (iterative calculation using the RLS algorithm). Matrix $\mathbf{F}$ and vector $\boldsymbol{\theta}$ are calculated using (2.19). Estimations of the unknown parameters are available in this step.

If any of the conditions in (3.2) holds, substitute $\mathbf{p}_0$ with $\mathbf{p}_0 + \widehat{\boldsymbol{\theta}}$ and then go to Step 1; otherwise, continue with Step 6.

Comments

From the viewpoint of online application, each of the steps is intended to be executed within one control cycle.

4. Evaluation of the RLS Algorithm by Simulation

The algorithm is evaluated using the data from simulation of an AFS/DYC-based integrated control system. Simulation of a double lane change maneuver is conducted using Matlab/Simulink. A nonlinear 8-DOF vehicle model along with a combined-slip tire model and a single-point preview driver model is used. Control commands are executed through correction steering angle on front wheels and brake torque applied on one of the four wheels.

The data for the steering angles at front wheels, brake torques on the four wheels, yaw rates, lateral acceleration, and vehicle speeds are used as inputs to the RLS based estimator. Estimated results of vehicle sideslip angles and road friction coefficients are compared with those from the simulation of double lane change maneuver using Matlab/Simulink. This enables the reader to evaluate whether the results are sufficiently precise to be used in control.

Two scenarios of double lane change maneuvers are involved: one is on high friction road surface and the other is on low friction road surface, and the target vehicle speeds for the two scenarios are 110 km/h and 40 km/h, respectively.

The initial sideslip angle and nominal tire-road friction coefficients on both sides are assumed to be 0, 0.8, and 0.8, respectively. The forgetting factor λ taking a value of 0.975 and σ in (2.19) is set to 1. The results are shown in Figures 5 and 6.

In each figure, the first one or two diagrams illustrate the inputs to the estimator. Estimated results are plotted in the second diagram, together with the actual data for comparison. When integrated control quits from intervention, the estimated sideslip angle and nominal tire-road friction coefficients are reset to their initial values. This is due to the fact that, with the current sensors onboard vehicles equipped with active safety systems, it is not possible to determine the surface coefficient of adhesion as long as vehicle remains within the linear range of operation [2].

For the double lane change maneuver performed on dry road with $\mu = 0.8$ and at 110 km/h, comparison of estimated and actual data in Figure 5 shows that the estimates of the yaw rate track the actual values with reasonable accuracy, and that the estimates of road friction coefficients are, on average, less than the actual values. However, the estimates of road friction coefficients can still provide useful information of road adhesion for the control

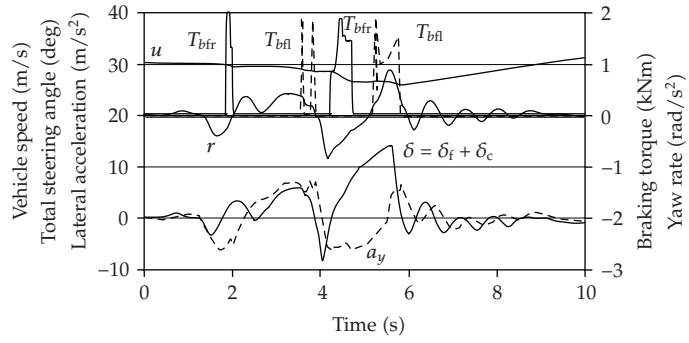

(a) Inputs to estimator

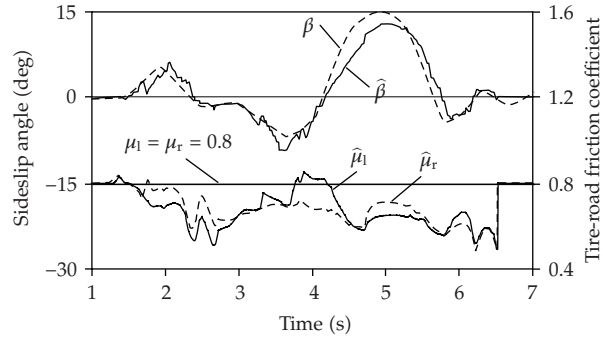

(b) Estimated results and comparison with actual data

Figure 5: Double lane change on high-μ at 110 km/h.

algorithm and are acceptable in the sense of road conditions in terms of slipperiness: normal ($\mu \geq 0.5$), slippery ($0.3 \leq \mu < 0.5$), and very slippery ($\mu < 0.3$) [3].

Figure 6 illustrates a double lane change maneuver performed on slippery road with $\mu = 0.2$ and at 40 km/h. This is a difficult maneuver from the estimation viewpoint, because of extremely slippery surface and low speed. Nevertheless, the estimates of the yaw rate and road friction coefficients track the actual values quite well during the maneuver. It is shown that the estimates of road friction after about 11s, when the double lane change maneuver has been completed, are not quite accurate. However, this inaccuracy has no adverse effect on control because information about the road friction within the linear range of operation is not required.

For evaluating the accuracy of the above estimated sideslip angle using the RLS algorithm, some results cited from [13] for a vehicle performing the same maneuver but using a methodology that combines a kinematic formulation and a state observer based on a single track vehicle model are shown in Figure 7 for comparison with the results shown in Figures 5(b) and 6(b). The results of Figure 7 show that the methodology used in [13] yields high accuracy of estimation. It is found from Figure 5(b) that when sideslip angle changes abruptly such as those from 4.2 s to 5.8 s, the estimate can not catch up with its actual value fast enough and thus a relatively large error arises. However, this error can be corrected by combining the proposed RLS algorithm with kinematic formulation, just like the methodology used in [13].

To evaluate robustness of the proposed RLS algorithm with repect to certain variantons that may occur during vehicle operation (mass, moment of inertia, tire cornering stiffness

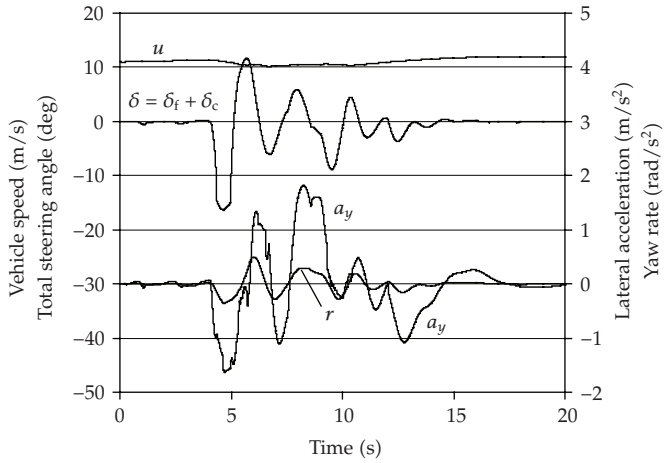

(a) Inputs to estimator (Part one)

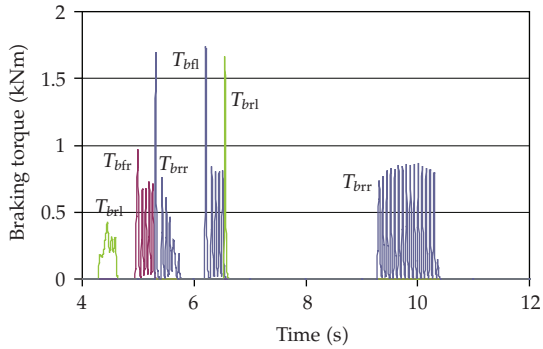

(b) Inputs to estimator (Part two)

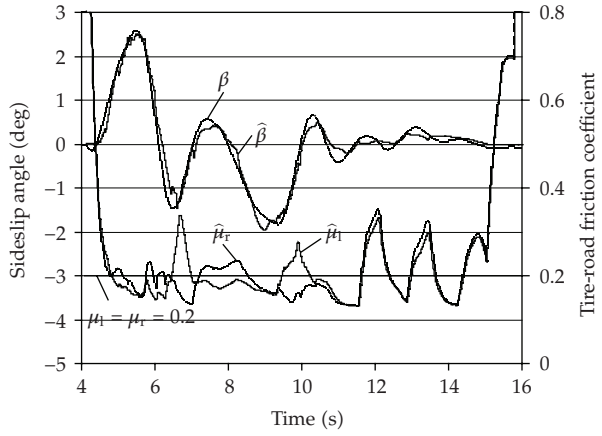

(c) Estimated results and comparison with actual data

Figure 6: Double lane change on low-μ at 40 km/h.

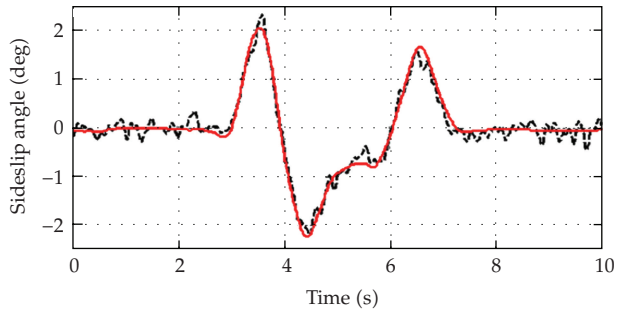

(a) On dry asphalt: 90 km/h, maximum a_y 6 m/s^2

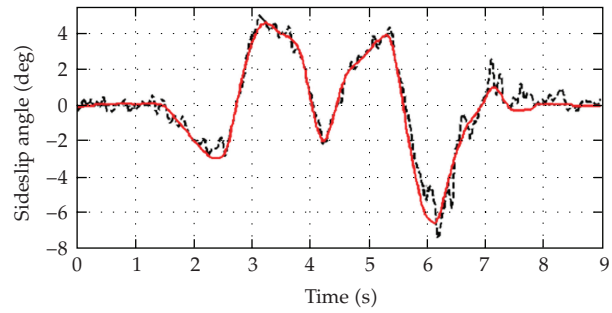

(b) On snow: 75 km/h, maximum a_y 3.8 m/s^2

Figure 7: Estimated results and comparison with experimental data for vehicle performing a double lane change maneuver, cited from [13].

etc.), more simulation was performed. As an example, Figure 8 illustrates the results obtained in a double lane change maneuver performed with different vehicle inertia properties. The vehicle inertia parameters are designated as $m = 1535\,\text{kg}$, $m_s = 1318\,\text{kg}$, $I_x = 445\,\text{kg·m}^2$, $I_z = 2513\,\text{kg·m}^2$ for the estimator, while those for the double lane change maneuver are $m = 1997\,\text{kg}$, $m_s = 1780\,\text{kg}$, $I_x = 601\,\text{kg·m}^2$, $I_z = 3269\,\text{kg·m}^2$. Though partly deviated from the actual states, the estimates are generally acceptable. In Figure 8a, the average estimated road friction coefficients deviate more from their actual values than those in Figure 5(b). For both cases shown in Figure 8, there are certain periods of time when the estimates of sideslip angle have a large error and lag, which indicates that the parameters for the algorithm should be further tuned to improve its robustness. Again, these errors appear during abrupt change of sideslip angle and can be reduced by combining the proposed RLS algorithm with kinematic formulation.

5. Conclusion

A model-based recursive least square algorithm for estimation of sideslip angle and road friction using data from the active front steering and dynamic yaw control logic is proposed.

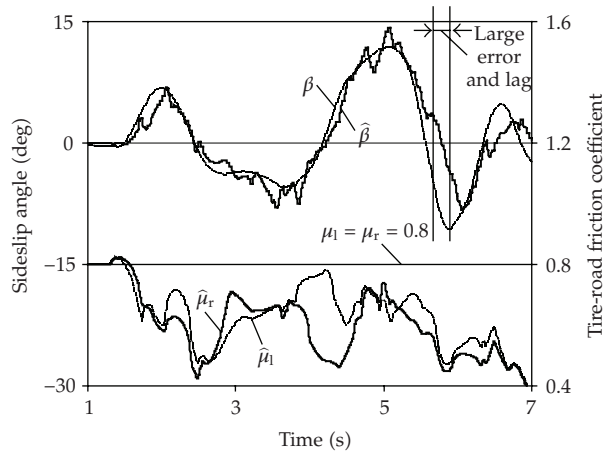

(a) Double lane change on high-μ at 110 km/h

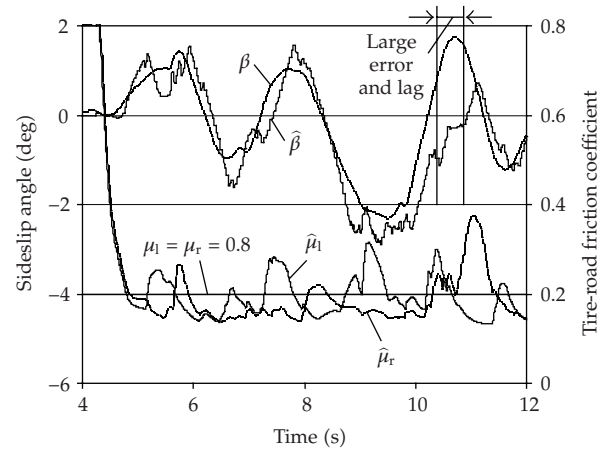

(b) Double lane change on low-μ at 38.5 km/h

Figure 8: Double lane change with variation of vehicle inertia properties

The estimates are evaluated through simulation of double lane change maneuvers using Matlab/Simulink. The results indicate that the strategy of estimation is valid and successful without using additional sensors, on both high and low friction road surfaces. Robustness of the algorithm is evaluated through more simulation with variation of vehicle inertia properties, and results show that the estimates are generally acceptable but the parameters for the algorithm need to be further tuned.

Though not yet included in our investigation, we propose that the RLS algorithm developed in this research be combined with kinematic formulation to enhance estimation accuracy during abrupt change of sideslip angle.

Future work of the research may include evaluation of the methodology through hardware-in-the-loop and road tests and implementation of the estimation algorithm on a vehicle stability enhancement system for online applications.

Nomenclature

Subscript, Abbreviation, and Symbol

fl: Front left
fr: Front right
rl: Rear left
rr: Rear right
f: Front
r: Rear
COG: Center of gravity
$\hat{}$: Indicator for estimated value
$\sim$: Indicator for error between measured and estimated values.

Parameters and Variables

a: Horizontal distance between vehicle COG and front axle
a_x: Longitudinal acceleration of vehicle
a_y: Lateral acceleration of vehicle
$\mathbf{B}$: Matrix for RLS algorithm
b: Horizontal distance between vehicle COG and rear axle
C_κ: Tire longitudinal slip stiffness
C_α: Tire cornering stiffness
D_y: Peak value of lateral force of tire
F_x: Longitudinal tire force in tire x-axis (of wheel plane)
F_{0y}: Lateral tire force in tire y-axis (of wheel plane) at pure-slip condition
F_y: Lateral tire force in tire y-axis (of wheel plane) at combined-slip condition
$F_{y\mathrm{p}}$: Peak value of lateral tire force in tire y-axis
$F_{y\mathrm{s}}$: Lateral tire force at pure lateral sliding in tire y-axis
F_z: Vertical force on tire
$F_{z\mathrm{s}}$: Vertical static force on tire
h_g: COG height of total vehicle mass with respect to ground
I_x: Roll moment of inertia (about vehicle x-axis)
I_z Yaw moment of inertia (about vehicle z-axis)
L: Wheel base
m: Total vehicle mass
m_{s}: Sprung mass of vehicle
r: Yaw rate
R_{w}: Tire static loaded radius
S_α: Tire lateral slip rate
$\mathbf{T_b}$: Brake torque vector for all the four wheels, defined as $\{T_{b\mathrm{fl}}, T_{b\mathrm{fr}}, T_{b\mathrm{rl}}, T_{b\mathrm{rr}}\}^T$
T_{b}: Brake torque on a single wheel
t: Time
t_{w}: Wheel track
u: Longitudinal velocity
V: Velocity vector at vehicle COG
v: Lateral velocity

$\mathbf{x}$: State vector
α: Tire sideslip angle
β: Vehicle sideslip angle at COG
δ: Total applied steer angle at wheels
δ_f: Applied steer angle at wheels, result of driver's input
δ_c: Correction steer angle at wheels supplied by AFS
κ: Longitudinal slip rate
ξ: Angle between velocity vector and vehicle x-axis
λ: Forgetting factor
$\boldsymbol{\theta}$: Parameter vector to be estimated
Φ: Index
μ: Tire-road nominal friction coefficient.

Acknowledgement

This work is supported by National Science Fund of China, with an approval number of 50475003.

References

[1] K. Yi, K. Hedrick, and S.-C. Lee, "Estimation of tire-road friction using observer based identifiers," *Vehicle System Dynamics*, vol. 31, no. 4, pp. 233–261, 1999.
[2] A. Hac and M. D. Simpson, "Estimation of vehicle sideslip angle and yaw rate," SAE Technical Paper Series 2000-01-0696, 2000.
[3] K. Li, J. A. Misener, and K. Hedrick, "On-board road condition monitoring system using slip-based tyre-road friction estimation and wheel speed signal analysis," *Proceedings of the Institution of Mechanical Engineers, Part K*, vol. 221, no. 1, pp. 129–146, 2007.
[4] U. Kiencke and A. Daiss, "Observation of lateral vehicle dynamic," *Control Engineering Practice*, vol. 5, no. 8, pp. 1045–1050, 1997.
[5] E. Esmailzadeh, A. Goodarzi, and G. R. Vossoughi, "Optimal yaw moment control law for improved vehicle handling," *Mechatronics*, vol. 13, no. 7, pp. 659–675, 2003.
[6] C. Canudas de Wit, H. Olsson, K. J. Åström, and P. Lischinsky, "A new model for control of systems with friction," *IEEE Transactions on Automatic Control*, vol. 40, no. 3, pp. 419–425, 1995.
[7] F. Gustafsson, "Slip-based tire-road friction estimation," *Automatica*, vol. 33, no. 6, pp. 1087–1099, 1997.
[8] L. Alvarez, J. Yi, R. Horowitz, and L. Olmos, "Dynamic friction model-based tyre-road friction estimation and emergency braking control," *ASME Journal of Dynamic Systems, Measurement, and Control*, vol. 127, no. 1, pp. 22–32, 2005.
[9] L. R. Ray, "Nonlinear tire force estimation and road friction identification: simulation and experiments," *Automatica*, vol. 33, no. 10, pp. 1819–1833, 1997.
[10] J. Yi, L. Alvarez, X. Claeys, and R. Horowitz, "Emergency braking control with an observer-based dynamic tire/road friction model and wheel angular velocity measurement," *Vehicle System Dynamics*, vol. 39, no. 2, pp. 81–97, 2003.
[11] T. A. Wenzel, K. J. Burnham, M. V. Blundell, and R. A. Williams, "Dual extended Kalman filter for vehicle state and parameter estimation," *Vehicle System Dynamics*, vol. 44, no. 2, pp. 153–171, 2006.
[12] G. Baffet, A. Charara, D. Lechner, and D. Thomas, "Experimental evaluation of observers for tire-road forces, sideslip angle and wheel cornering stiffness," *Vehicle System Dynamics*, vol. 46, no. 6, pp. 501–520, 2008.
[13] F. Cheli, E. Sabbioni, M. Pesce, and S. Melzi, "A methodology for vehicle sideslip angle identification: comparison with experimental data," *Vehicle System Dynamics*, vol. 45, no. 6, pp. 549–563, 2007.
[14] T. Shim and D. Margolis, "Model-based road friction estimation," *Vehicle System Dynamics*, vol. 41, no. 4, pp. 249–276, 2004.

[15] U. Eichhorn and J. Roth, "Prediction and monitoring of tyre-road friction," in *Proceedings of the 24th Congress on Safety, the Vehicle, and the Road (FISTA '92)*, vol. 2, pp. 67–74, 1992.

[16] B. Breuler, U. Eichhorn, and J. Roth, "Measurement of tyre-road friction ahead of the car and inside the tyre," in *Proceedings of the International Symposium on Advanced Vehicle Control (AVEC '92)*, pp. 347–353, Yokohama, Japan, September 1992.

[17] T. Bachmann, "The importance of the integration of road, tyre, and vehicle technologies," in *Proceedings of 20th World Congress on Federation of Societies of Automobile Engineering (FISITA '95)*, Montreal, Canada, 1995.

[18] B. Breuer, M. Bartz, B. Karlheinz, et al., "The mechatronic vehicle corner of Darmstadt University of technology-interaction and cooperation of a sensor tire, new low-energy disc brake and smart wheel suspension," in *Proceedings of the International Federation of Societies of Automobile Engineering (FISITA '00)*, Seoul, Korea, June 2000, Paper F2000G281.

[19] S. Müller, M. Uchanski, and K. Hedrick, "Estimation of the maximum tyre-road friction coefficient," *Journal of Dynamic Systems, Measurement, and Control*, vol. 125, pp. 607–617, 2003.

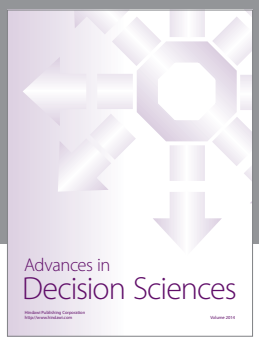

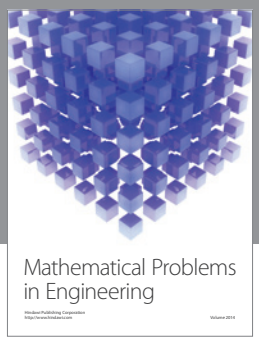

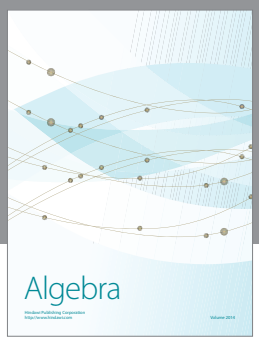

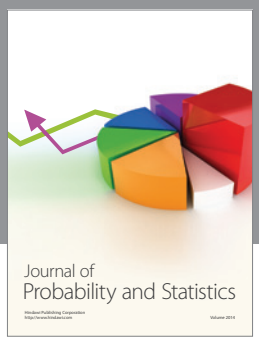

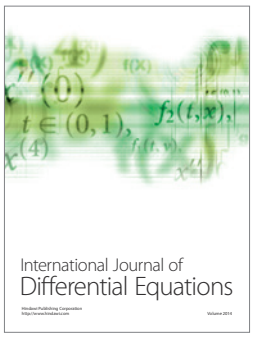

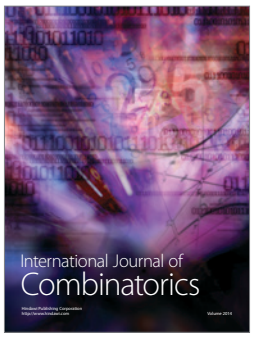

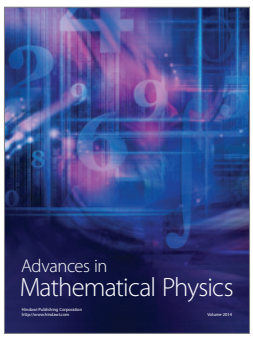

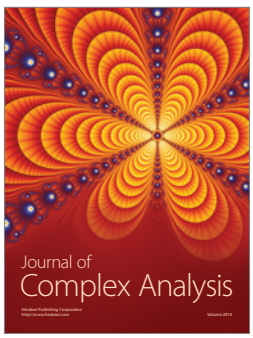

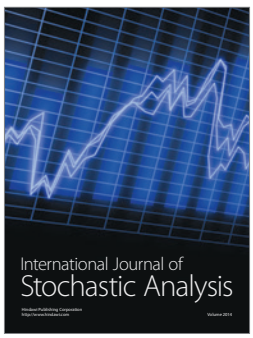

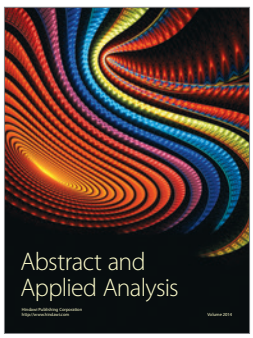

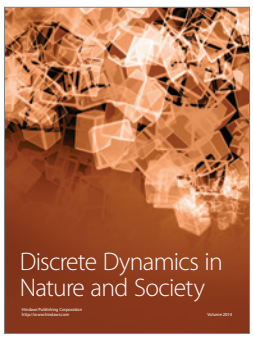

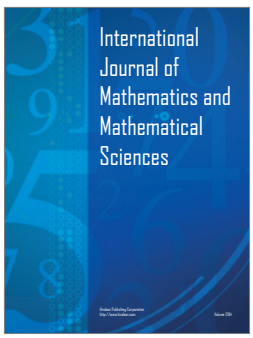

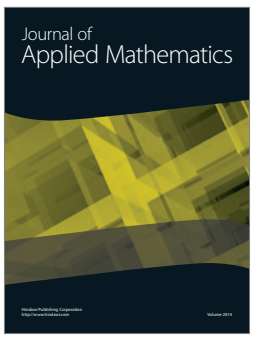

Hindawi
Submit your manuscripts at
http://www.hindawi.com